This is the accepted manuscript made available via CHORUS. The article has been published as:

Suppression of electronic correlations by chemical pressure from FeSe to FeS

P. Reiss, M. D. Watson, T. K. Kim, A. A. Haghighirad, D. N. Woodruff, M. Bruma, S. J. Clarke, and A. I. Coldea

Phys. Rev. B **96**, 121103 — Published 5 September 2017

DOI: 10.1103/PhysRevB.96.121103

Suppression of electronic correlations by chemical pressure from FeSe to FeS

P. Reiss,[1] M. D. Watson,[2] T. K. Kim,[2] A. A. Haghighirad,[1] D. N. Woodruff,[3] M. Bruma,[1] S. J. Clarke,[3] and A. I. Coldea[1,*]

[1]*Clarendon Laboratory, Department of Physics, University of Oxford, Parks Road, Oxford OX1 3PU, UK*
[2]*Diamond Light Source, Harwell Campus, Didcot, OX11 0DE, UK*
[3]*Department of Chemistry, University of Oxford, Inorganic Chemistry Laboratory, South Parks Road, Oxford, OX1 3QR, United Kingdom*

(Dated: August 16, 2017)

Iron-based chalcogenides are complex superconducting systems in which orbitally-dependent electronic correlations play an important role. Here, using high-resolution angle-resolved photoemission spectroscopy, we investigate the effect of these electronic correlations outside the nematic phase in the tetragonal phase of superconducting $FeSe_{1-x}S_x$ ($x = 0, 0.18, 1$). With increasing sulfur substitution, the Fermi velocities increase significantly and the band renormalizations are suppressed towards a factor of $1.5-2$ for FeS. Furthermore, the chemical pressure leads to an increase in the size of the quasi-two dimensional Fermi surface, compared with that of FeSe, however, it remains smaller than the predicted one from first-principle calculations for FeS. Our results show that the isoelectronic substitution is an effective way to tune electronic correlations in $FeSe_{1-x}S_x$, being weakened for FeS with a lower superconducting transition temperature. This suggests indirectly that electronic correlations could help to promote higher-T_c superconductivity in FeSe.

Iron-based superconductors offer an interesting playground to explore the competition of low-energy electronic ground states, such as superconductivity, spin-density wave and nematic states. These low-energy electronic states are strongly influenced by the presence of the different $3d$ orbitals of Fe, the Hund's coupling, Coulomb interactions and band filling [1, 2]. The orbitally-selective nature of these interactions often leads to different bandwidth renormalizations and an unusual relative energy shift of various bands with respect to each other and the Fermi level due to the pronounced particle-hole asymmetry of the electronic structure [3]. Iron-chalcogenides are among the most correlated iron-based superconductors, displaying the largest spread of orbitally-dependent bandwidth renormalization. The most pronounced renormalization is observed for the band with d_{xy} orbital character, reaching a factor of 17 and being sensitive to the isoelectronic substitution, as for $FeSe_{1-x}Te_x$ [4, 5].

FeSe is a unique system in which the role of correlations on nematicity and superconductivity can be explored, in the absence of a competing long-range spin-density wave order. Superconductivity in FeSe around $T_c \approx 9$ K emerges out of a nematic electronic state, showing strong anisotropy in the electronic and superconducting properties [6–8]. The origin of this nematic phase below $T_s \approx 90$ K, which coincides with a tetragonal-orthorhombic structural phase transition [9], is the orbital order that breaks the four-fold rotational symmetry and thus leads to the lifting of the d_{xz}/d_{yz} orbital degeneracy [6, 10]. Previous studies in the tetragonal phase found orbitally-dependent band renormalizations for FeSe reaching values from 3-4 for the degenerate d_{xz}/d_{yz} bands, to 7-9 for the d_{xy} band [6, 11]. Furthermore, the strength of electronic correlations manifests by the existence of a lower Hubbard band at large binding energies, recently detected in FeSe [12, 13].

Superconductivity in bulk FeSe can be strongly enhanced using various tuning parameters, such as applied physical pressures [14, 15], chemical intercalations [16] and *in-situ* potassium dosing [17]. The enhancement in superconductivity by doping of the surface [17] was found to be directly linked to the increase of electronic correlations. However, sulfur substitution in $FeSe_{1-x}S_x$ completely suppresses the nematic state for $x \geq 0.18(1)$ [6, 18, 19], without promoting a high-T_c superconducting phase or stabilizing a magnetic order, in contrast to applied pressure [14, 15]. The end member of this series, the tetragonal FeS, with a lower $T_c \approx 4$ K, is suggested to be less correlated [20, 21], emphasizing the important role of chemical pressure in tuning electronic ground states and the strength of electronic correlations.

In this paper, we study the suppression of electronic correlations and the changes in band structure as a function of isoelectronic substitution in the tetragonal phase of $FeSe_{1-x}S_x$ using high-resolution angle-resolved photoemission spectroscopy (ARPES). The low-temperature Fermi surface of the tetragonal phase with $x = 0.18$ resembles that of FeSe at high temperatures ($T > T_s$), and it expands towards FeS, but it does not reach the size predicted by first-principle calculations. The Fermi velocities increase and the band renormalizations decrease significantly with increasing x. At the same time, superconductivity is weakened as the electronic correlations of the d_{xz}/d_{yz} bands are reduced from a factor of 3–4 for FeSe ($T_c \approx 9$ K) to 1.5–2 for FeS ($T_c \approx 4$ K).

Experimental details $FeSe_{1-x}S_x$ single crystals with x=0 and x=0.18 were grown by the $KCl/AlCl_3$ chemical vapor transport method [22, 23]. FeS and other single crystals with $0.5 \leq x \leq 1$ were grown by the hydrothermal method, using $K_{0.8}Fe_{1.6}(Se_{1-x}S_x)_2$ precursors [24]. ARPES measurements were performed at the I05 beamline at the Diamond Light Source [25], using horizontally and vertically linearly-polarized synchrotron light (LH and LV) between 20 and 120 eV, with ≈6 to 19 meV resolution. Band structure calculations for FeS were performed with Wien2K using GGA, spin-orbit coupling and experimental lattice parameters, (a = 3.6802(5) Å, c = 5.0307(7) Å and z_S = 0.2523 [24]).

Hole bands of tetragonal $FeSe_{1-x}S_x$. Fig. 1(a)-(c) com-

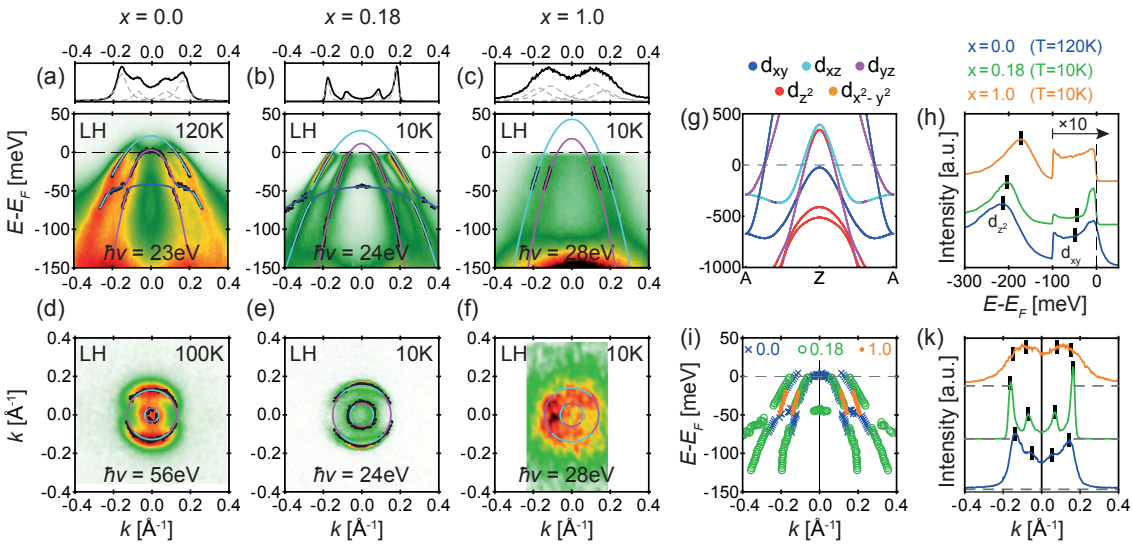

FIG. 1. **The hole bands of tetragonal $FeSe_{1-x}S_x$ ($x = 0, 0.18, 1$).** The ARPES spectra for a) FeSe at 120 K (as in Ref.[6]), b) x=0.18 at 10 K and c) FeS at 10 K centered at high symmetry Z-point. d)-f) The corresponding maps for the same compounds, as above. g) Band structure calculations for FeS using experimental parameters. h) Energy distribution curves (EDCs) and k) momentum distribution curves (MDCs) for the three compounds. i) Extracted peak positions from fits to the MDCs from a)-c) for the hole bands at the Z-point.

pares the hole band dispersions at the top of the Brillouin zone, centered at the Z point, in the tetragonal phase of FeSe at 120 K ($T > T_s$) with those of x=0.18 and FeS at 10 K. The photon energies corresponding to high-symmetry points along k_z were established by analysis of the d_{z^2} intensity well below E_F, shown in Fig.SM1 in the Supplemental Material (SM) [26]. Despite the significant amount of sulfur substitution in x=0.18, the linewidths of the band dispersions in the ARPES spectra remain narrow due to the high quality of these crystals, that also allows quantum oscillations to be observed [19]. This is in contrast to the much broader ARPES spectrum of FeS, shown in Fig. 1(c), likely caused by the larger degree of disorder in crystals grown by the hydrothermal method with residual resistivity ratios varying between 5 to 17 (Fig. 3(e)).

Band dispersions and the Fermi surface maps in Fig. 1 show that the high-T band structure of FeSe and the low-T band structure of x=0.18 are very similar, confirming the absence of the nematic state for x=0.18 at 10 K. The shape of the Fermi surface is isotropic in the $k_x - k_y$ plane for all three compositions (Fig. 1 (d)-(f)), in contrast to the elliptical Fermi surface found in the nematic phase of FeSe [27] and for $x \leq 0.15$ [18]. Two hole-like dispersions cross the Fermi level close to the Z point, separated only by the spin-orbit coupling estimated to $\sim$ 20 meV in FeSe [6, 28].

For a quantitative analysis of the band structure, band positions were extracted by performing simultaneous constrained Lorentzian fits to the momentum distribution curves (MDC) for different light polarizations at a fixed energy, shown in Fig. 1(i) and (k). For FeS, best fits were obtained also using two hole-like bands at the Fermi level, as expected from the band structure calculations (Fig. 1(g)), even though the two bands are harder to separate (see also Fig.SM3 in SM [26]). We find a measurable increase of the k_F values and the Fermi surface areas with increasing S substitution (Fig. 1(i)), in agreement with the trends found in quantum oscillations up to $x \approx 0.19$ [19].

One unusual feature of the electronic structure of FeSe is the existence of a small 3D hole pocket centered only around the Z point at 120 K (Fig. 1(a) and (d)). This innermost hole band is pushed below the Fermi level at low temperatures, due to the combined effects of orbital order and spin-orbit coupling [18, 29], whereas at high temperatures chemical potential shifts may occur [30]. As orbital ordering is reduced with S substitution, this small 3D pocket reappears at Z for $x \sim 0.11$ at low temperatures [18], consistent with our observations for $x = 0.18$ (Fig. 1(b) and (e) and Fig.SM3). However, in FeS, due to the significant increase in bandwidths, we find that this pocket has become two-dimensional, as evidenced by two bands crossing the Fermi level both at the Γ and Z point (Fig.SM3). This finding agrees with the larger anisotropy reported for FeS, as compared with FeSe [21].

Next, we compare the change in the electronic correlations as a function of S substitution. The strongest renormalizations are expected for bands with d_{xy} character, but in ARPES, they are notoriously difficult to observe due to matrix element effects and the suppression of the spectral weight with the increase in the electronic correlations, as observed in $FeSe_xTe_{1-x}$ [31]. However, their dispersions can be revealed due to band hybridization caused by the spin-orbit coupling effects [3, 6, 27, 32]. This allows us to identify the d_{xy} hole band in FeSe and $FeSe_{0.82}S_{0.18}$, and we find it significantly pushed below the Fermi level ($\sim$ 50 meV), in contrast to band structure calculations where it crosses the Fermi level (see Fig. SM2 in SM [26]). In FeS, the d_{xy} band is not resolved

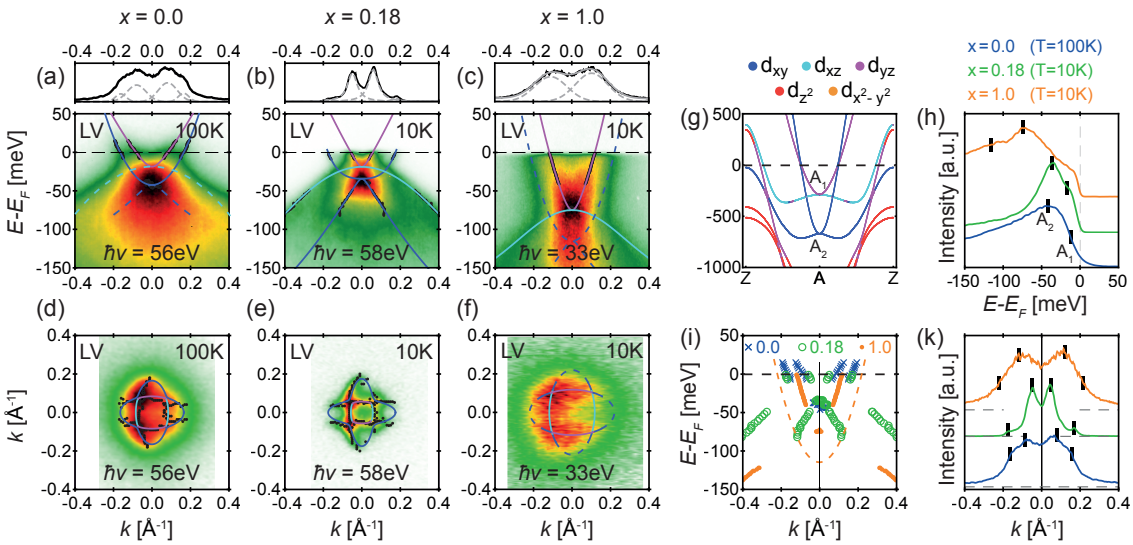

FIG. 2. **The electron bands of tetragonal $FeSe_{1-x}S_x$ ($x = 0, 0.18, 1$).** a-c) ARPES intensity plots of the band structure through the A point and d)-f) the corresponding maps for the three compounds, as in Fig. 1. g) Band structure calculations for FeS using experimental parameters. h) EDCs and k) MDCs for the three compounds. i) Extracted peak positions from fits to the MDCs from a)-c).

due mainly to disorder effects, as found in other iron-based superconductors [33],

In FeSe, the d_{xy} band renormalization is rather large (a factor 7-9), in contrast to the d_{xz}/d_{yz} band renormalization (a factor 3-4) [6, 11] and we find that they do not change significantly when comparing to x=0.18, shown in Fig. 1(i). However, for FeS we extract a significantly reduced band renormalization of 1.7(1) for the d_{xz}/d_{yz} bands, reflecting moderate electronic correlations for FeS with a low $T_c \sim 4$ K. In addition, d_{z^2} band lies closer to the Fermi level (≈ 150 meV), as compared with DFT (350 meV) or FeSe (210 meV in Fig. 1(h)), suggestive of finite correlation effects in FeS (renormalized by a factor ≈ 2 from the k_z dependence in Fig.SM1 in SM [26]). Furthermore, the Fermi velocities v_F extracted from the band dispersion slopes (Fig. 1(i) and Fig. 3(d)) significantly increase from FeSe towards FeS, whereas the quasiparticle effective masses, $m^\star$, of the outer hole-like bands decrease from 3-4 m_e for $x = 0.18$ to 1-2 m_e for FeS. These findings agree with the reduction of the effective masses detected in quantum oscillations studies in $FeSe_{1-x}S_x$ (outside the nematic phase) [19] and in FeS [21].

Electron bands of tetragonal $FeSe_{1-x}S_x$. Fig. 2(a)-(c) compares the evolution of the band structure at the A point in the tetragonal phase of FeSe at 100 K, and of x=0.18 and FeS at 10 K. As for the hole-like bands at the Z point, the ARPES spectra of FeSe and $FeSe_{0.82}S_{0.18}$ are very similar, confirming that for $x \sim 0.18$, the Fermi surface deformation observed in the nematic state of FeSe is completely suppressed [6, 18]. The spectra of all samples display two electron-like bands crossing the Fermi level, but they are much harder to separate for FeS (Fig.SM3 in SM [26]). For FeS we use a single band fit to the MDCs in Fig.2(k), whereas the outer electron band size with d_{xy} character is affected by matrix elements and disorder effects. Fermi surface maps in Fig. 2(d-f) display a four-fold symmetric shape, with small differences between the inner electron-like Fermi surface pocket between x=0.18 and FeSe at 100 K, whereas a significant expansion is detected for FeS (Fig. 2(f)).

At the corners of the tetragonal Brillouin zone, there are two degenerate states, A_1 and A_2 (Fig.2(g)), which are the bottom of the inner and outer electron bands and are not split by the spin-orbit interaction [29]. The increased separation between these states upon cooling through the nematic transition has caused a significant debate about the origin of the nematic phase [13, 27–29]. Here we find the bottom of the inner electron band is $\approx 19(5)$ meV below the Fermi level for x=0 and x=0.18 (Fig.2(h) and (i)), with slight variation for the outer electron band ($\approx 42(5)$ meV for x=0 and $\approx 34(5)$ meV for x=0.18). A small variation in the position of the bands could originate due to the slight temperature variation of lattice parameters, as we compare the high temperature spectra for FeSe with the low-temperature spectra for x=0.18. Notably in FeS, these two degenerate states are significantly lower in energy compared with the other two compositions ($\approx$ 70 meV and $\approx$ 120 meV, respectively), a direct consequences of the increased bandwidths (identified from the energy distribution curves (EDC) shown in Fig. 2(h)). This extended bandwidth, in conjunction with the equally significant increase of the Fermi velocity (Fig. 2(i) and Fig. 3(d)) and a decrease of the quasiparticle effective masses, highlight the significant reduction in the electronic correlations in FeS, in particular, when comparing with x=0.18 outside the nematic phase.

The phase diagram of $FeSe_{1-x}S_x$ together with the evolution of the Fermi surface in the tetragonal phase from FeSe to FeS is shown in Fig.3(c) and Fig.3(a), respectively. While

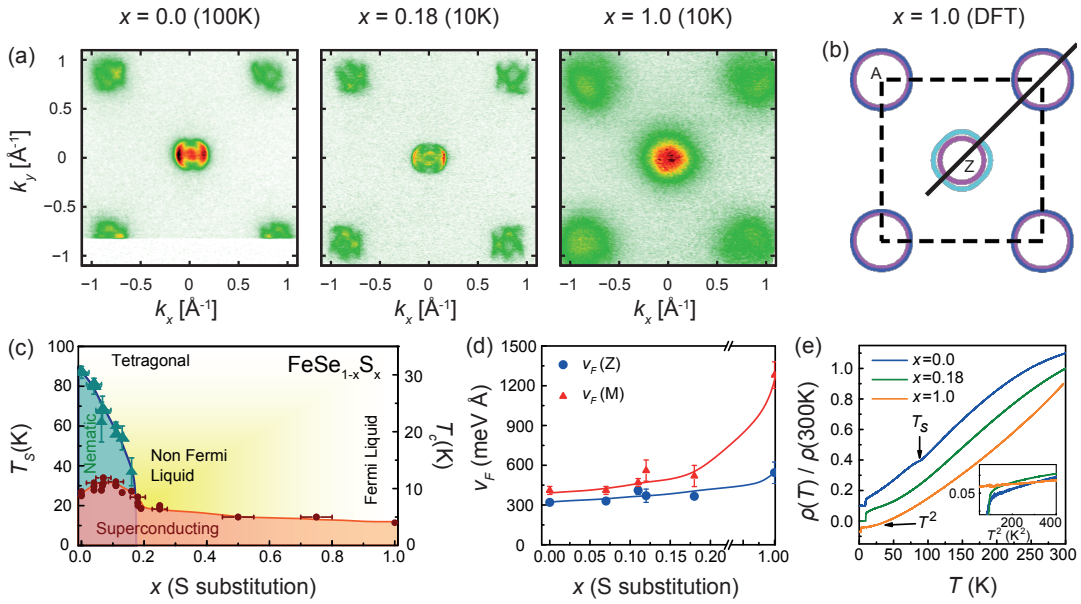

FIG. 3. **Phase diagram of $FeSe_{1-x}S_x$ and the suppression of electronic correlations by S substitution.** a) The ARPES map of the high-symmetry cut through top of the Brillouin zone for the tetragonal phase of $FeSe_{1-x}S_x$ (x=0, 0.18, 1) at 56-69 eV, together with a calculated slice for FeS in b). The solid line indicates the cuts used during ARPES experiments. c) Proposed phase diagram of $FeSe_{1-x}S_x$, including different transport and thermodynamic measurements from Refs.[19, 34, 35]. d) The evolution of the Fermi velocities as a function of chemical pressure. e) The temperature dependence of resistivity of $FeSe_{1-x}S_x$ (x=0, 0.18, 1) showing strong deviations of resistivity from T^2 Fermi liquid behavior for low sulfur substitution. The data are renormalized to the room temperature values and shifted for clarity.

the size of the quasi-two dimensional Fermi surface increases with chemical pressure, the most important change is the increase in Fermi velocities (and bandwidths) (Fig.3(d)), which reflects the reduction of the electronic correlations. These findings agree with the reduction of the effective masses determined from quantum oscillations in $FeSe_{1-x}Se_x$ outside the nematic phase [19, 36] and FeS [20, 21]. Furthermore, the low temperature resistivity shows a T^2 Fermi-liquid-like behavior for FeS, in contrast to the other compositions closer to the nematic phase, as shown in Fig.3(e) and also reported in Ref.[37]. The low-T_c superconductivity in $FeSe_{1-x}S_x$ has a small dome inside the nematic region, being gently suppressed towards FeS (Fig.3(c)). This behavior is in contrast to FeSe under applied pressure [38] or *in-situ* K dosing [17], where superconductivity is enhanced once the nematic phase is suppressed, with an additional magnetic phase being stabilized under pressure [14, 15, 38].

Our results on the electronic structure of FeS are in good agreement with a recent ARPES study [39]. Quantum oscillations in FeS reported only small frequencies below 200 T [21], a factor 2.5 smaller than the smallest area of the inner hole band predicted by band structure calculations [19]. Our ARPES data do not reveal the presence of such a small band (with a $k_F \sim 0.0780$Å^{-1}), but we note that the d_{xy} band is not visible in our data due to the matrix effects, impurity line broadening or loss of spectral weight. This d_{xy} band is predicted by DFT calculations to lie very close to the Fermi level in FeS (Fig. 1f). Furthermore, due to the complex de-intercalation procedure to prepare FeS, other byproducts could form [40]. Recently, a quantum oscillations study suggested that FeS has a 3D Fermi surface [20], not supported by the current ARPES studies.

As FeS remains in the tetragonal phase and the electronic correlations are reduced, one would expect a better agreement between the experimental and calculated Fermi surface of FeS (see Fig.3(b)). However, we find that the Fermi surface areas and the quasiparticle masses of FeS are still a factor $\sim$ 2 smaller than predicted by DFT calculations (Fig.3b and Fig.SM2 in SM [26]). This band shrinking thus also manifests in FeS, but is weaker than in FeSe [6]. Furthermore, FeS is reminiscent of other iron-based superconductors with a low T_c, LaFePO and LiFeP, where the renormalization effects extracted from quantum oscillations were rather moderate ($\approx$ 2) [41, 42]. Interestingly, all these end member compounds, LaFePO and LiFeP and FeS, display nodal superconductivity [43–46] and the pnictogen and chalcogen position is closer to the iron planes compared to their isoelectronic sister-compounds. These trends have been captured theoretically by Kuroki *et al.* [47], where the height of the pnictogen acts as a switch between high-T_c nodeless and low-T_c nodal pairings and that superconductivity is suppressed once the lattice constants are reduced, as in the case of FeS. Substituting smaller S ions onto the Se site shrinks the unit cell [24, 34], decreases the Fe chalcogen bond lengths and brings the chalcogen closer to the iron planes. This would result in a greater orbital overlap causing an increase in the bandwidth and the degree of electronic correlations will reduced significantly, like in FeS.

Summary. Our high-resolution ARPES study on

$FeSe_{1-x}S_x$ single crystals reveal the suppression of the electronic correlations, demonstrated by the increase in Fermi velocities and bandwidth, while the superconductivity is weakened away from the nematic phase. The chemical pressure effects in $FeSe_{1-x}S_x$ lead to the increase in the size of the quasi-two dimensional Fermi surface, however, its size still remains smaller than predicted from first principle band structure calculations. Our results suggest that electronic correlations may be important for enhancing superconductivity in iron-based superconductors and chemical pressure offers an ideal tuning parameter to control them.

Acknowledgements We thank Moritz Hoesch for technical support. This work was mainly supported by EPSRC (EP/L001772/1, EP/I004475/1, EP/I017836/1). A.A.H. acknowledges the financial support of the Oxford Quantum Materials Platform Grant (EP/M020517/1). We thank Diamond Light Source for access to Beamline I05 (proposal number SI15471) that contributed to the results presented here. The authors would like to acknowledge the use of the University of Oxford Advanced Research Computing (ARC) facility in carrying out part of this work. A.I.C. acknowledges an EPSRC Career Acceleration Fellowship (EP/I004475/1) and thanks hospitality of KITP supported by the National Science Foundation under Grant No. NSF PHY-1125915.

* corresponding author:amalia.coldea@physics.ox.ac.uk

[1] Z. P. Yin, K. Haule, and G. Kotliar, "Kinetic frustration and the nature of the magnetic and paramagnetic states in iron pnictides and iron chalcogenides." Nat. Mater. **10**, 932–5 (2011).

[2] Luca de' Medici, Gianluca Giovannetti, and Massimo Capone, "Selective Mott Physics as a Key to Iron Superconductors," Phys. Rev. Lett. **112**, 177001 (2014).

[3] L. Fanfarillo, J. Mansart, P. Toulemonde, H. Cercellier, P. Le Fèvre, F. Bertran, B. Valenzuela, L. Benfatto, and V. Brouet, "Orbital-dependent Fermi surface shrinking as a fingerprint of nematicity in FeSe," Phys. Rev. B **94**, 155138 (2016).

[4] Ming Yi, Zhongkai Liu, Yan Zhang, Rong Yu, Jianxin Zhu, James Lee, Rob Moore, Felix Schmitt, Wei Li, Scott Riggs, Jiun-Haw Chu, Bing Lv, Jin Hu, Makoto Hashimoto, Sung-Kwan Mo, Zahid Hussain, Zhiqiang Mao, Ching-Wu Chu, Ian Fisher, Qimiao Si, Zhi-Xun Shen, and Donghui Lu, "Observation of universal strong orbital-dependent correlation effects in iron chalcogenides," Nat. Comm. **6**, 7777 (2015).

[5] A. Tamai, A. Y. Ganin, E. Rozbicki, J. Bacsa, W. Meevasana, P. D. C. King, M. Caffio, R. Schaub, S. Margadonna, K. Prassides, M. J. Rosseinsky, and F. Baumberger, "Strong Electron Correlations in the Normal State of the Iron-Based $FeSe_{0.42}Te_{0.58}$ Superconductor Observed by Angle-Resolved Photoemission Spectroscopy," Phys. Rev. Lett. **104**, 097002 (2010).

[6] M. D. Watson, T. K. Kim, A. A. Haghighirad, N. R. Davies, A. McCollam, A. Narayanan, S. F. Blake, Y. L. Chen, S. Ghannadzadeh, A. J. Schofield, M. Hoesch, C. Meingast, T. Wolf, and A. I. Coldea, "Emergence of the nematic electronic state in FeSe," Phys. Rev. B **91**, 155106 (2015).

[7] M. A. Tanatar, A. E. Böhmer, E. I. Timmons, M. Schütt, G. Drachuck, V. Taufour, K. Kothapalli, A. Kreyssig, S. L. Bud'ko, P. C. Canfield, R. M. Fernandes, and R. Prozorov, "Origin of the Resistivity Anisotropy in the Nematic Phase of FeSe," Phys. Rev. Lett. **117**, 127001 (2016).

[8] P. O. Sprau, A. Kostin, A. Kreisel, A. E. Böhmer, V. Taufour, P. C. Canfield, S. Mukherjee, P. J. Hirschfeld, B. M. Andersen, and J. C. Séamus Davis, "Discovery of Orbital-Selective Cooper Pairing in FeSe," arXiv , 1611.02134 (2016).

[9] T. M. McQueen, A. J. Williams, P. W. Stephens, J. Tao, Y. Zhu, V. Ksenofontov, F. Casper, C. Felser, and R. J. Cava, "Tetragonal-to-Orthorhombic Structural Phase Transition at 90 K in the Superconductor $Fe_{1.01}Se$," Phys. Rev. Lett. **103**, 057002 (2009).

[10] T. Shimojima, Y. Suzuki, T. Sonobe, A. Nakamura, M. Sakano, J. Omachi, K. Yoshioka, M. Kuwata-Gonokami, K. Ono, H. Kumigashira, A. E. Böhmer, F. Hardy, T. Wolf, C. Meingast, H. V. Löhneysen, H. Ikeda, and K. Ishizaka, "Lifting of xz/yz orbital degeneracy at the structural transition in detwinned FeSe," Phys. Rev. B **90**, 121111 (2014).

[11] J. Maletz, V. B. Zabolotnyy, D. V. Evtushinsky, S. Thirupathaiah, A. U. B. Wolter, L. Harnagea, A. N. Yaresko, A. N. Vasiliev, D. A. Chareev, A. E. Böhmer, F. Hardy, T. Wolf, C. Meingast, E. D. L. Rienks, B. Büchner, and S. V. Borisenko, "Unusual band renormalization in the simplest iron-based superconductor FeSe," Phys. Rev. B **89**, 220506 (2014).

[12] Matthew D. Watson, Steffen Backes, Amir A. Haghighirad, Moritz Hoesch, Timur K. Kim, Amalia I. Coldea, and Roser Valentí, "Formation of Hubbard-like bands as a fingerprint of strong electron-electron interactions in FeSe," Phys. Rev. B **95**, 081106 (2017).

[13] D. V. Evtushinsky, M. Aichhorn, Y. Sassa, Z.-H. Liu, J. Maletz, T. Wolf, A. N. Yaresko, S. Biermann, S. V. Borisenko, and B. Buchner, "Direct observation of dispersive lower Hubbard band in iron-based superconductor FeSe," arXiv:1612.02313 (2016).

[14] S. Medvedev, T. M. McQueen, I. A. Troyan, T Palasyuk, M I Eremets, R J Cava, S Naghavi, F Casper, V Ksenofontov, G Wortmann, and C Felser, "Electronic and magnetic phase diagram of β-$Fe_{1.01}Se$ with superconductivity at 36.7 K under pressure," Nat. Mater. **8**, 630 (2009).

[15] Taichi Terashima, Naoki Kikugawa, Shigeru Kasahara, Tatsuya Watashige, Takasada Shibauchi, Yuji Matsuda, Thomas Wolf, Anna E. Böhmer, Frédéric Hardy, Christoph Meingast, Hilbert v. Löhneysen, and Shinya Uji, "Pressure-Induced Antiferromagnetic Transition and Phase Diagram in FeSe," J. Phys. Soc. Japan **84**, 063701 (2015).

[16] M. Burrard-Lucas, D. G. Free, S. J. Sedlmaier, J. D. Wright, S. J. Cassidy, Y. Hara, A. J. Corkett, T. Lancaster, P. J. Baker, S. J. Blundell, and S. J. Clarke, "Enhancement of the superconducting transition temperature of FeSe by intercalation of a molecular spacer layer," Nat. Mat. **12**, 15 (2013).

[17] C. H. P. Wen, H. C. Xu, C. Chen, Z. C. Huang, X. Lou, Y. J. Pu, Q. Song, B. P. Xie, Mahmoud Abdel-Hafiez, D. A. Chareev, A. N. Vasiliev, R. Peng, and D. L. Feng, "Anomalous correlation effects and unique phase diagram of electron-doped FeSe revealed by photoemission spectroscopy," Nat. Commun. **7**, 10840 (2016).

[18] M. D. Watson, T. K. Kim, A. A. Haghighirad, S. F. Blake, N. R. Davies, M. Hoesch, T. Wolf, and A. I. Coldea, "Suppression of orbital ordering by chemical pressure in $FeSe_{1-x}S_x$," Phys. Rev. B **92**, 121108 (2015).

[19] A. I. Coldea, S. F. Blake, S. Kasahara, A. A. Haghighirad, M. D. Watson, W. Knafo, E. S. Choi, A. McCollam, P. Reiss, T. Yamashita, M. Bruma, S. Speller, Y. Matsuda,

T. Wolf, T. Shibauchi, and A. J. Schofield, "Evolution of the Fermi surface of the nematic superconductors $FeSe_{1-x}S_x$," arXiv:1611.07424 (2017).

[20] Haoran Man, Jiangang Guo, Rui Zhang, Rico Schönemann, Zhiping Yin, Mingxuan Fu, Matthew B. Stone, Qingzhen Huang, Yu Song, Weiyi Wang, David J. Singh, Felix Lochner, Tilmann Hickel, Ilya Eremin, Leland Harriger, Jeffrey W. Lynn, Collin Broholm, Luis Balicas, Qimiao Si, and Pengcheng Dai, "Spin excitations and the Fermi surface of superconducting FeS," npj Quantum Mat. **2** (2017).

[21] Taichi Terashima, Naoki Kikugawa, Hai Lin, Xiyu Zhu, Hai-Hu Wen, Takuya Nomoto, Katsuhiro Suzuki, Hiroaki Ikeda, and Shinya Uji, "Upper critical field and quantum oscillations in tetragonal superconducting FeS," Phys. Rev. B **94**, 100503 (2016).

[22] Dmitriy Chareev, Evgeniy Osadchii, Tatiana Kuzmicheva, Jiunn-Yuan Lin, Svetoslav Kuzmichev, Olga Volkova, and Alexander Vasiliev, "Single crystal growth and characterization of tetragonal $FeSe_{1-x}$ superconductors," Cryst. Eng. Comm. **15**, 1989 (2013).

[23] A. E. Böhmer, V. Taufour, W. E. Straszheim, T. Wolf, and P. C. Canfield, "Variation of transition temperatures and residual resistivity ratio in vapor-grown FeSe," Phys. Rev. B **94**, 024526 (2016).

[24] Xiaofang Lai, Hui Zhang, Yingqi Wang, Xin Wang, Xian Zhang, Jianhua Lin, and Fuqiang Huang, "Observation of Superconductivity in Tetragonal FeS," J. Am. Chem. Soc. **137**, 10148–10151 (2015), http://dx.doi.org/10.1021/jacs.5b06687.

[25] M. Hoesch, T. K. Kim, P. Dudin, H. Wang, S. Scott, P. Harris, S. Patel, M. Matthews, D. Hawkins, S. G. Alcock, T. Richter, J. J. Mudd, M. Basham, L. Pratt, P. Leicester, E. C. Longhi, A. Tamai, and F. Baumberger, "A facility for the analysis of the electronic structures of solids and their surfaces by synchrotron radiation photoelectron spectroscopy," Rev. Sci. Inst. **88**, 013106 (2017).

[26] See Supplemental Material at [URL will be inserted by publisher] for additional ARPES analysis, raw ARPES data at different high symmetry points and first-principle band structue calculations for FeSe and FeS.

[27] M. D. Watson, T. K. Kim, L. C. Rhodes, M. Eschrig, M. Hoesch, A. A. Haghighirad, and A. I. Coldea, "Evidence for unidirectional nematic bond ordering in FeSe," Phys. Rev. B **94**, 201107 (2016).

[28] Matthew D. Watson, Amir A. Haghighirad, Hitoshi Takita, Wumiti Mansuer, Hideaki Iwasawa, Eike F. Schwier, Akihiro Ino, and Moritz Hoesch, "Shifts and Splittings of the Hole Bands in the Nematic Phase of FeSe," J. Phys. Soc. Jpn. **86**, 053703 (2017), http://dx.doi.org/10.7566/JPSJ.86.053703.

[29] Rafael M. Fernandes and Oskar Vafek, "Distinguishing spin-orbit coupling and nematic order in the electronic spectrum of iron-based superconductors," Phys. Rev. B **90**, 214514 (2014).

[30] L. C. Rhodes, M. D. Watson, A. A. Haghighirad, M. Eschrig, and T. K. Kim, "Strongly enhanced temperature dependence of the chemical potential in FeSe," Phys. Rev. B **95**, 195111 (2017).

[31] Z. K. Liu, M. Yi, Y. Zhang, J. Hu, R. Yu, J.-X. Zhu, R.-H. He, Y. L. Chen, M. Hashimoto, R. G. Moore, S.-K. Mo, Z. Hussain, Q. Si, Z. Q. Mao, D. H. Lu, and Z.-X. Shen, "Experimental observation of incoherent-coherent crossover and orbital-dependent band renormalization in iron chalcogenide superconductors," Phys. Rev. B **92**, 235138 (2015).

[32] A. Fedorov, A. Yaresko, T. K. Kim, Y. Kushnirenko, E. Haubold, T. Wolf, M. Hoesch, A. Grüneis, B. Büchner, and S. V. Borisenko, "Effect of nematic ordering on electronic structure of FeSe," Sci. Rep. **6**, 36834 (2016).

[33] Z. R. Ye, Y. Zhang, F. Chen, M. Xu, J. Jiang, X. H. Niu, C. H. P. Wen, L. Y. Xing, X. C. Wang, C. Q. Jin, B. P. Xie, and D. L. Feng, "Extraordinary doping effects on quasiparticle scattering and bandwidth in iron-based superconductors," Phys. Rev. X **4**, 031041 (2014).

[34] Y. Mizuguchi, F. Tomioka, S. Tsuda, T. Yamaguchi, and Y. Takano, "Substitution Effects on FeSe Superconductor," J. Phys. Soc. Jpn. **78**, 074712 (2009), http://dx.doi.org/10.1143/JPSJ.78.074712.

[35] Mahmoud Abdel-Hafiez, Yuan-Yuan Zhang, Zi-Yu Cao, Chun-Gang Duan, G. Karapetrov, V. M. Pudalov, V. A. Vlasenko, A. V. Sadakov, D. A. Knyazev, T. A. Romanova, D. A. Chareev, O. S. Volkova, A. N. Vasiliev, and Xiao-Jia Chen, "Superconducting properties of sulfur-doped iron selenide," Phys. Rev. B **91**, 165109 (2015).

[36] P. Reiss, D. Graf, A. A. Haghighirad, P. Cai, M. Bristow, and A. I. Coldea, in preparation (2017).

[37] Takahiro Urata, Yoichi Tanabe, Khuong Kim Huynh, Hidetoshi Oguro, Kazuo Watanabe, and Katsumi Tanigaki, "Non-Fermi liquid behavior of electrical resistivity close to the nematic critical point in $Fe_{1-x}Co_xSe$ and $FeSe_{1-y}S_y$," arXiv , 1608.01044 (2017).

[38] J. P. Sun, K. Matsuura, G. Z. Ye, Y. Mizukami, M. Shimozawa, K. Matsubayashi, M. Yamashita, T. Watashige, S. Kasahara, Y. Matsuda, J.-Q. Yan, B. C. Sales, Y. Uwatoko, J.-G. Cheng, and T. Shibauchi, "Dome-shaped magnetic order competing with high-temperature superconductivity at high pressures in FeSe," Nat. Commun. **7**, 12146 (2016).

[39] J. Miao, X. H. Niu, D. F. Xu, Q. Yao, Q. Y. Chen, T. P. Ying, S. Y. Li, Y. F. Fang, J. C. Zhang, S. Ideta, K. Tanaka, B. P. Xie, D. L. Feng, and Fei Chen, "Electronic structure of FeS," arXiv.1703.08682 (2017).

[40] Franziska K. K. Kirschner, Franz Lang, Craig V. Topping, Peter J. Baker, Francis L. Pratt, Sophie E. Wright, Daniel N. Woodruff, Simon J. Clarke, and Stephen J. Blundell, "Robustness of superconductivity to competing magnetic phases in tetragonal FeS," Phys. Rev. B **94**, 134509 (2016).

[41] A. I. Coldea, J. D. Fletcher, A. Carrington, J. G. Analytis, A. F. Bangura, J.-H. Chu, A. S. Erickson, I. R. Fisher, N. E. Hussey, and R. D. McDonald, "Fermi Surface of Superconducting LaFePO Determined from Quantum Oscillations," Phys. Rev. Lett. **101**, 216402 (2008).

[42] C. Putzke, A. I. Coldea, I. Guillamón, D. Vignolles, A. McCollam, D. LeBoeuf, M. D. Watson, I. I. Mazin, S. Kasahara, T. Terashima, T. Shibauchi, Y. Matsuda, and A. Carrington, "de Haas-van Alphen Study of the Fermi Surfaces of Superconducting LiFeP and LiFeAs," Phys. Rev. Lett. **108**, 047002 (2012).

[43] J. D. Fletcher, A. Serafin, L. Malone, J. G. Analytis, J.-H. Chu, A. S. Erickson, I. R. Fisher, and A. Carrington, "Evidence for a nodal-line superconducting state in LaFePO," Phys. Rev. Lett. **102**, 147001 (2009).

[44] K. Hashimoto, S. Kasahara, R. Katsumata, Y. Mizukami, M. Yamashita, H. Ikeda, T. Terashima, A. Carrington, Y. Matsuda, and T. Shibauchi, "Nodal versus Nodeless Behaviors of the Order Parameters of LiFeP and LiFeAs Superconductors from Magnetic Penetration-Depth Measurements," Phys. Rev. Lett. **108**, 047003 (2012).

[45] Jie Xing, Hai Lin, Yufeng Li, Sheng Li, Xiyu Zhu, Huan Yang, and Hai-Hu Wen, "Nodal superconducting gap in tetragonal FeS," Phys. Rev. B **93**, 104520 (2016).

[46] Yang Yang, Wan-Sheng Wang, Hong-Yan Lu, Yuan-Yuan Xiang, and Qiang-Hua Wang, "Electronic structure and $d_{x^2-y^2}$-wave superconductivity in FeS," Phys. Rev. B **93**, 104514

(2016).
[47] Kazuhiko Kuroki, Hidetomo Usui, Seiichiro Onari, Ryotaro Arita, and Hideo Aoki, "Pnictogen height as a possible switch between high-T_c nodeless and low-T_c nodal pairings in the iron-based superconductors," Phys. Rev. B **79**, 224511 (2009).